J Fluoresc (2010) 20:243–250
DOI 10.1007/s10895-009-0545-0

ORIGINAL PAPER

Fluorescent Method for the Determination of Sulfide Anion with ZnS:Mn Quantum Dots

Bao-Hua Zhang · Fang-Ying Wu · Yu-Mei Wu · Xun-Shou Zhan

Received: 15 July 2009 / Accepted: 15 September 2009 / Published online: 30 September 2009

Abstract Water-soluble Mn^{2+}-doped ZnS quantum dots (QDs) were prepared using mercaptoacetic acid as the stabilizer. The optical properties and structure features were characterized by X-Ray, absorption spectrum, IR spectrum and fluorescence spectrum. In pH 7.8 Tris-HCl buffer, the QDs emitted strong fluorescence peaked at 590 nm with excitation wavelength at 300 nm. The presence of sulfide anion resulted in the quenching of fluorescence and the intensity decrease was proportional to the S^{2-} concentration. The linear range was from 2.5×10^{-6} to 3.8×10^{-5} mol L^{-1} with detection limit as 1.5×10^{-7} mol L^{-1}. Most anions such as F^-, Cl^-, Br^-, I^-, $CH_3CO_2^-$, ClO_4^-, CO_3^{2-}, NO_2^-, NO_3^-, $S_2O_3^{2-}$, SO_3^{2-} and SO_4^{2-} did not interfere with the determination. Thus a highly selective assay was proposed and applied to the determination of S^{2-} in discharged water with the recovery of ca. 103%.

Keywords ZnS:Mn^{2+} nanocrystals · Quantum dots · Sulfide anion · Fluorescence quenching

Introduction

The risk of sulfide anion toxicity is associated with exposure in a number of occupational settings [1–3]. Continuous and high concentration exposure of sulfide can cause various physiological and biochemical problems. When sulfide anion is protonated, it becomes even more toxic. Thus the detection of sulfide anion has become very important from industrial, environmental, and biological point of view [4]. Many methods have been developed so far including titration [5], spectrophotometry [6–10], inductively coupled plasma atomic emission spectroscopy (ICP-AES) [11], hydride generation atomic fluorescence spectrometry (HGAFS) [12], electrochemical methods [13–16], ion chromatography [17, 18], chemiluminescence (CL) methods [4, 19–21] and fluorimetry [22–26]. Among them, fluorimetry has received considerable attention because of high sensitivity and easy detection. Recently semiconductor nanocrystals or quantum dots (QDs) have been widely used because they offer many advantages over conventional organic fluorophores due to their generally high luminescence quantum yield, good photochemical stability, broad excitation band and narrow emission band, size-dependent emission wavelength and large effective Stokes shift [27]. They are most frequently used to detect cations [28–35]. Recently, they have been applied to the detection of anions as well. Lakowicz et al. [36] reported the detection of I^- by surface modified CdS. Alfredo et al. [37, 38] reported the selective determination of CN^- in methanol by tert-butyl-N-(2-mercaptoethyl)-carbamate modified CdSe QDs. Liu et al. [39] developed a new method to detect NO_2^- by CdSe QDs. Wu et al. [40] realized the highly selective detection of HSe^- by water soluble CdS QDs with slight interference from Cu^{2+} and S^{2-}. Multrooney et al. [41] detected F^- by CdSe/ZnS QDs. Usually the fluorescence emission of doping ions has higher photostability than the defect-related luminescence of semiconductive nanomaterials, because the defects are greatly affected by synthesis conditions and environments. Because of its wide band gap (3.7 eV), zinc sulfide (ZnS) is particularly suitable for

B.-H. Zhang · F.-Y. Wu (✉) · X.-S. Zhan
Department of Chemistry and Center of Analysis and Testing,
Nanchang University,
Nanchang 330031, China
e-mail: fywu@ncu.edu.cn

Y.-M. Wu
Packaging Engineering Institute of Jinan University,
Zhuhai 519070, China

use as a host material for a large variety of dopants. Mn^{2+}-doped ZnS had strong orange emission at ca. 600 nm and high quantum yield [42–46].The luminescence lifetime of Mn^{2+}-doped ZnS nanocrystals was ca. 1 ms. Such a long lifetime made the luminescence from the nanocrystal readily distinguishable from the background luminescence [47]. Therefore Mn^{2+}-doped ZnS nanocrystals have been extensively used as fluorescent sensor in various applications. Tu et al. [48] synthesized the amine-capped Mn^{2+}-doped ZnS nanocrystals for the ultra sensitive detection of 2,4,6-trinitrotoluene(TNT) in liquid and gas explosive substance. Yan et al. [49] applied the phosphoresence of ZnS:Mn^{2+} to the assay of enoxacin in biological fluids. Wang et al. [50] proposed an assay for pentachlorophenol based on SiO_2 modified ZnS:Mn^{2+}. Swadeshmukul et al. [51] synthesized water soluble mercaptoacetic CdS/ZnS:Mn^{2+} QDs which were used in biological imaging. However until now the detection of sulfide anion by QDs has never been reported yet. Herein, we synthesized mercaptoacetic coated ZnS:Mn^{2+} QDs which showed excellent water solubility and optical properties. At the same time, the QDs highly selectively responded to sulfide anion in pH 7.8 Tris-HCl buffer.

Experimental

Apparatus

All fluorescence measurements were carried out on a F-4600 spectrofluorimeter (Hitachi, Japan) equipped with a xenon lamp source and a 1.0 cm quartz cell, both slits of emission and excitation were 5 nm and the scan speed was 1,200 nm min^{-1}. Absorption spectra were recorded on a Shimadzu-2501 UV-Vis spectrophotometer (Shimadzu

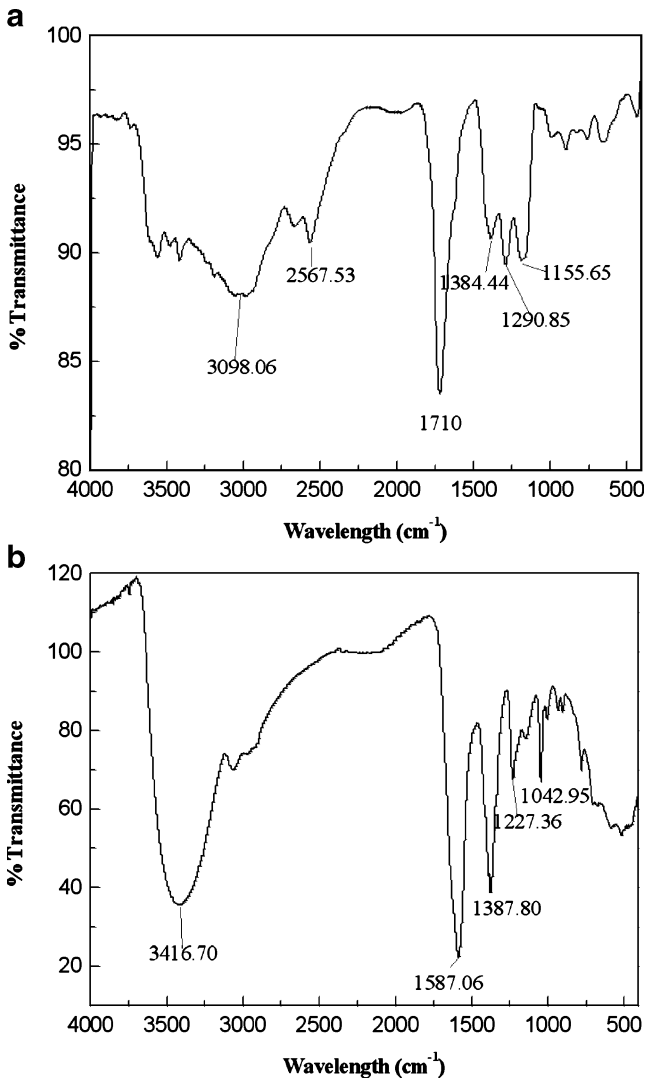

Fig. 1 FTIR spectra of mercaptoacetic acid(TGA) (**a**) and TGA capped QDs (**b**)

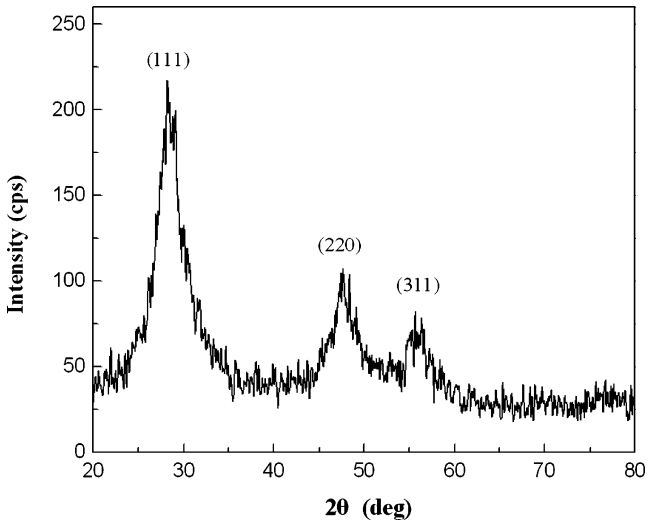

Fig. 2 The XRD patterns of ZnS:Mn^{2+} nanocrystal powders

Japan) using a 1.0 cm quartz cell. X-ray spectroscopy was collected on XRD DI SYSTEM (Bede England). Infrared spectra were obtained as KBr pellets on a Nicolet 5700 FTIR spectrometer. Size distribution of ZnS:Mn^{2+} was performed on Hydrosol Nano-particle size analyzer and Zeta Potential Analyzer (PSA NANO2590, Malvern Companies, UK). The multi-elemental analysis of ZnS:Mn^{2+} QDs was performed on ICP-AES OPTIMA 5300DV (Perkin-Elmer,U.S.A). All pH measurements were made with a pHS-3 digital pH-meter (Shanghai REX Instrument Corp., Shanghai, China) with a combined glass-calomel electrode.

Reagents

All chemicals were of analytical grade and were used without further purification. All solutions were prepared using doubly distilled water. $Zn(CH_3CO_2)_2{\bullet}2H_2O$ and $Mn(CH_3CO_2)_2{\bullet}\ 4H_2O$ were the products of the Shanghai Qingxi Technology Co., Ltd., $NaS{\bullet}9H_2O$ was purchased from Shanghai Chemical Technology Development Co., Ltd., Tris (Sigma Chemical Co.) buffer had a pH of 7.8. The sodium salts of the tested anions and the chloride of the tested cations were Sigma-Aldrich Corp. products.

Preparation of mn-doped ZnS QDs [52]

To the three-necked flask, 5.0 mL of 0.1 mol L^{-1} Zn $(CH_3CO_2)_2$, 20 mL of 0.1 mol L^{-1} mercaptoacetic acid and 1.5 mL of 0.01 mol L^{-1} $Mn(CH_3CO_2)_2$ were added and diluted to 50 mL with doubly deionized water. The pH of the mixed solution was adjusted to be 10.5 using 2.0 mol L^{-1} NaOH and nitrogen gas was passed for 30 min at room temperature in order to remove oxygen. Then, 5.0 ml of 0.1 mol L^{-1} Na_2S was quickly injected into the solution under vigorous stirring under nitrogen atmosphere for 15 min. At last, the solution was aged at 50 °C in air for 2 h. The aged solution was precipitated with anhydrous ethanol, the precipitate was centrifuged and washed with ethanol, then dried in vacuum. The ZnS:Mn^{2+} nanocrystals were obtained.

Procedure of measurement

A certain amount of ZnS:Mn^{2+} powder was dispersed in deionized water and the solution of 100 μg mL^{-1} was obtained. Different concentrations of sulfide anion were added into 0.6 mL QDs solution and diluted to 2.0 ml with Tris-HCl aqueous solution of pH 7.8. The fluorescence spectra were obtained with excitation wavelength at 300 nm. The scan speed was 1,200 nm min^{-1} and the band-slits of both excitation and emission were set as 5.0 nm.

Results and discussion

IR spectra of mercaptoacetic acid and ZnS:Mn^{2+} QDs capped TGA

The IR spectra of mercaptoacetic acid (TGA) and QDs capped with TGA were shown in Fig. 1. It was clear that the absorption band at 2,567 cm^{-1} which was ascribed to sulfhydryl group disappeared in the spectrum of QDs. The asymmetric and symmetric stretch vibrations of the carboxyl group of TGA were at 1,710 cm^{-1} and 1,384.4 cm^{-1} respectively. After binding to QDs, they shifted to 1,587.1 cm^{-1} and 1,387.8 cm^{-1} respectively. It could be concluded that mercaptoacetic acid has bound to the surface of QDs. As a result, the solubility of QDs in water was improved.

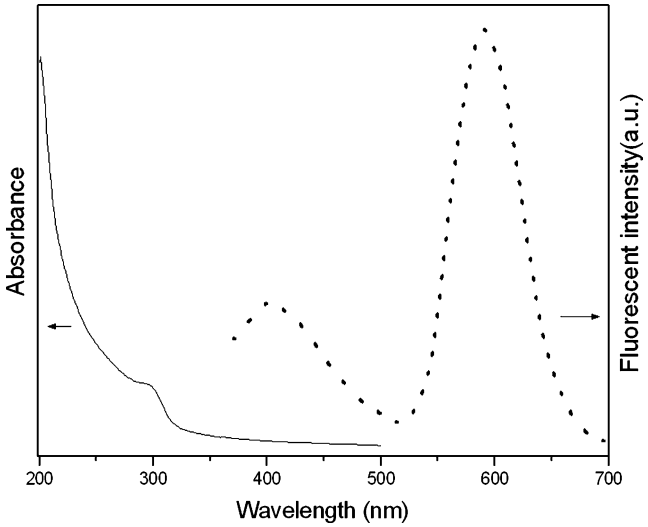

Fig. 3 UV absorption spectrum (*solid line*) and fluorescence spectrum (*dot line*) of Mn-doped ZnS QDs in aqueous solution

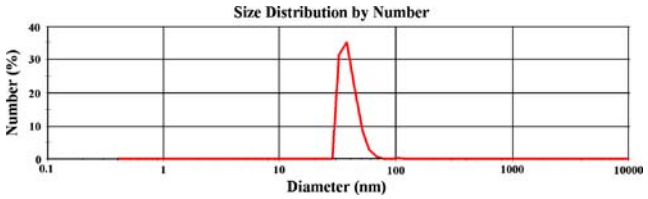

Fig. 4 Size distribution by number of ZnS:Mn^{2+} Hydrosol

Content of doped manganese

The amount of Mn doped will affect the fluorescent intensity of QDs. The experiment results displayed that the optimal molar ratio between Mn^{2+} and Zn^{2+} was 0.03 in synthesis of Mn-Doped ZnS QDs. The actual concentration ratio of Mn^{2+} and Zn^{2+} was 0.028 which was obtained from inductively coupled plasma analyzer (ICP).

Characterization of the Mn-doped ZnS QDs by XRD

For different drying condition under 60 °C, 120 °C and 210 °C, the XRD spectra of QDs showed no significant discrepancy. Figure 2 presented the XRD patterns of ZnS:Mn^{2+} QDs which were obtained under 210 °C for drying. These diffraction features appealing at 28.5°, 47.5°, and 56.3° corresponded to the (111), (220), and (311) planes of cubic sphalerite ZnS, which was very consistent with the values in the standard card (PDF-card 5-566). It implied that the Mn-doped ZnS possessed the cubic sphalerite ZnS crystal model. According to Debye-Scherrer formula,

$$D = k\lambda/\beta\cos(\theta) \quad (1)$$

where D is the averaged crystallite size, λ is the wavelength of X-ray, usually using line K_α of Cu with wavelength of 0.15,406 nm, θ is a glancing angle between X-rays and a crystal face, k is a constant as 0.89, andβis the full width at half maximum of the diffraction line. From the equation (1), D of Mn-doped ZnS was estimated as 3.8 nm.

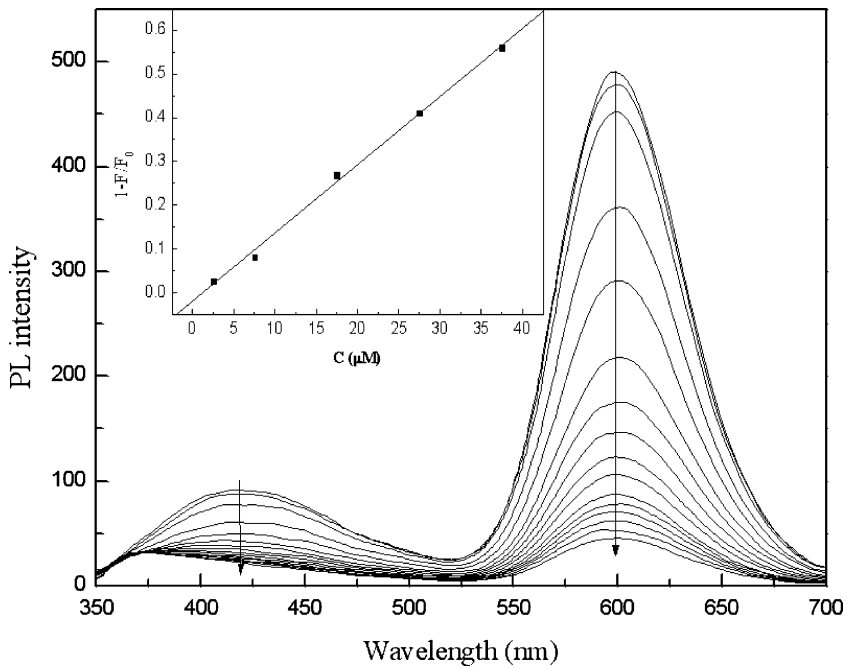

Fig. 5 Fluorescent spectral changes of QDs in pH 7.8 Tris-HCl buffer upon addition of S^{2-}. The excitation wavelength was 300 nm. The inset was the fitted liner relationship between intensity ratio and concentration of S^{2-}. The concentration of S^{2-} was 0, 0.25, 0.75, 1.75, 2.75, 3.75, 4.75, 5.75, 6.75, 7.75, 8.75, 9.75, 11.75, and 13.75×10^{-5} mol L^{-1}, respectively. Arrow indicants increasing of S^{2-} concentration

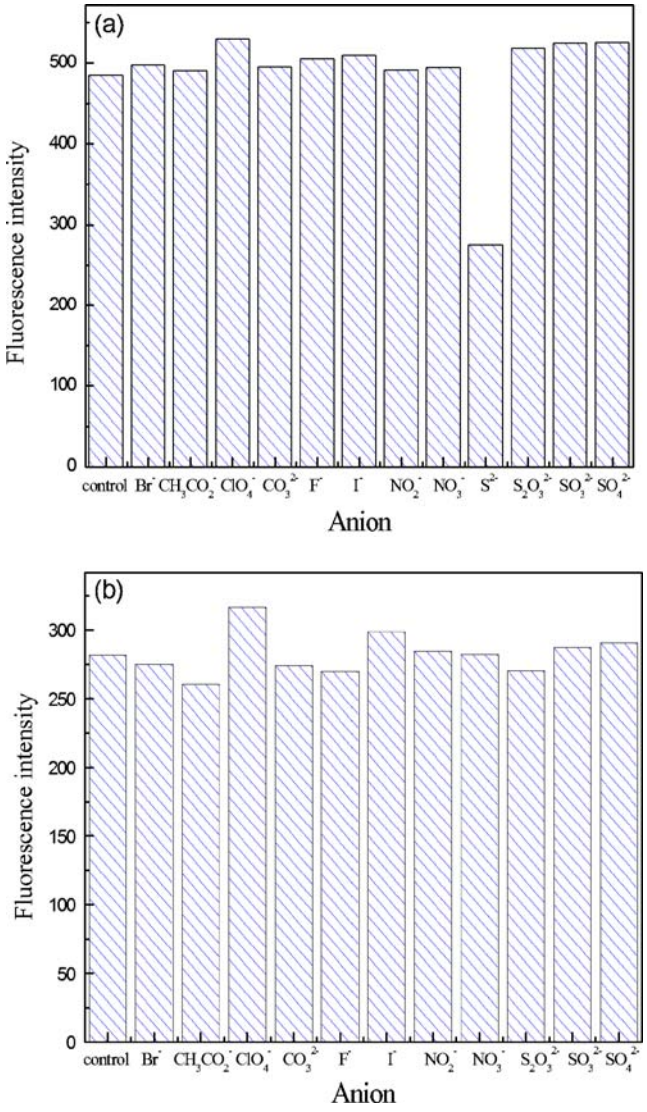

Fig. 6 **a** Intensity change of QDs (30 μg mL^{-1}) in the presence and absence of anions. The concentration of sulfide anion was 2.5×10^{-5}mol L^{-1} while the concentrations of other anions were 2.5×10^{-4}mol L^{-1}. **b** The intensity change of QDs and 2.5×10^{-5}mol L^{-1} sulfide anion mixture upon addition of different anions (2.5×10^{-4}mol L^{-1})

Spectroscopic properties of ZnS:Mn^{2+} QDs in aqueous solution

The fluorescence spectrum and absorption spectrum of ZnS:Mn^{2+} QDs in pH 7.8 aqueous solution were presented in Fig. 3. The absorption peak was 294 nm (4.22 eV) which showed the band gap absorption of ZnS:Mn^{2+} nanocrystalline particles. Compared with the phase material of ZnS whose absorption peak was at 340.6 nm (3.64 eV), the absorption peak blue shifted 46 nm (0.58 eV). The result indicated that ZnS:Mn^{2+}possessed quantum confinement effect. According to Brus effective mass approximation [53], the average size of ZnS:Mn^{2+} was estimated as 4.1 nm which was consistent with the result of XRD. Two emission bands peaked at 400 nm and 590 nm, respectively were observed when excitation wavelength set at 300 nm. The weak emission at 400 nm originated from the defect-related emission of the ZnS [54]. The strong emission peak at 590 nm is attributed to the $^4T_1-^6A_1$ transition of Mn^{2+} impurity which indicated Mn^{2+} entered into the ZnS lattice to form ZnS: Mn^{2+} QDs. However, the green fluorescence at 480 nm of ZnS phase wasn't observed which was attributed to energy transfer from ZnS QDs to Mn^{2+} [48].

Size distribution of ZnS:Mn^{2+} hydrosol

In order to explore the emission mechanism, the size of QDs in aqueous solution was measured. As described in the section of procedure of measurement, the nanocrystal hydrosol was prepared and the size distribution curve was presented in Fig. 4. It was clear that the size of nanocrytal concentrated in the range of 33–50 nm. The narrow scope suggested the nanocrystal hydrosol was relatively uniform in size distribution. Placed the nanocrystal hydrosol in the refrigerator at 4 °C for 3 days, no observable precipitation

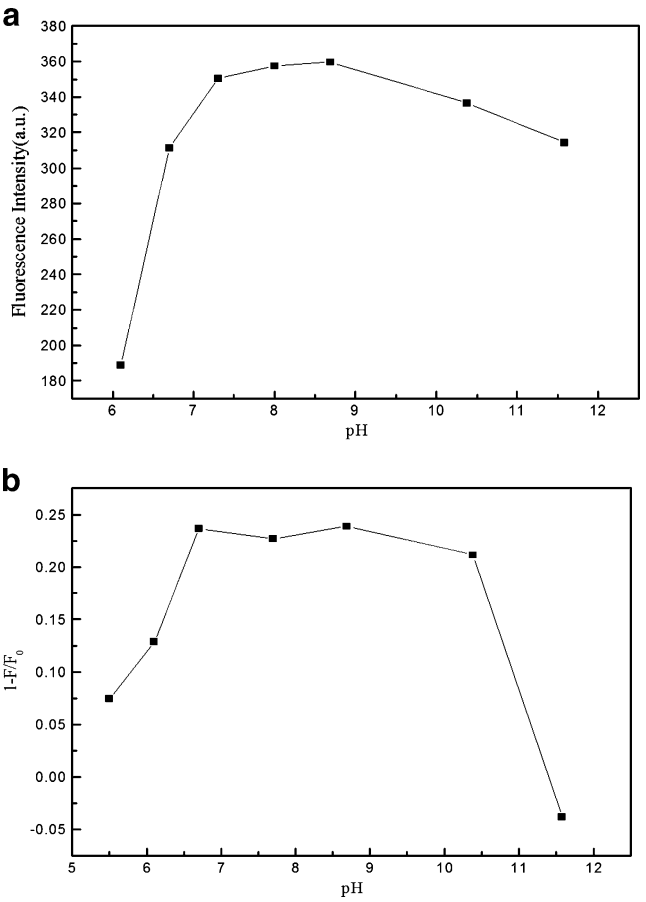

Fig. 7 **a** Effect of pH on the fluorescence intensity of QDs (30 μg mL^{-1}), **b** the fluorescent intensity change of system containing QDs (30 μg mL^{-1}) and S^{2-} (1.5×10^{-5}mol L^{-1}) in different pH solution

was found and the size distribution curve kept constant. Such a transparent solution implied that Mn-doped ZnS nanocrystal has good water solubility and stability which was promising for the application. Obviously, the size of the hydrated molecule was significantly larger than that of solid owing to the hydration of nanocrystal hydrosol. But the emission profile and peak position in solid state and in hydrosol solution were the same which implied that the hydration action did not change the luminescent properties of QDs.

Spectral changes of ZnS: Mn^{2+} QDs in the presence of anions

Figure 5 showed the fluorescent spectrum changes of QDs upon addition of S^{2-}. In the pH 7.8 Tris-HCl buffer, the addition of S^{2-} resulted in the fluorescence quenching. The fluorescence quenching was best described by the equation:$1-F/F_0=-0.018+0.016[Q]$, where F_0 and F were the fluorescent intensity of QDs in the absence and presence of S^{2-}, [Q] was the concentration of the quencher (S^{2-}). The linear relationship of the intensity ratio vs S^{2-} concentration was presented in the insert of Fig. 5. The linear range of the calibration curve was from 2.5×10^{-6} to 3.8×10^{-5}mol L^{-1} with the detection limit as 1.5×10^{-7}mol L^{-1}.

In the above quenching experiment, the excitation wavelength was set at 300 nm. However, the absorbance of ca. 300 nm increased upon addition of S^{2-}. It was concluded that the fluorescence quenching of QDs upon addition of S^{2-} was ascribed to be the binding action between QDs and S^{2-} instead of the change of absorbance.

The effect of various anions on the fluorescence spectrum of ZnS:Mn^{2+} QDs was also investigated and presented in Fig. 6. Upon the presence of 2.5×10^{-4}mol L^{-1} for each anion such as Cl^-, Br^-, $CH_3CO_2^-$, ClO_4^-, CO_3^{2-}, F^-, I^-, NO_2^-, NO_3^-, $S_2O_3^{2-}$, SO_3^{2-} and SO_4^{2-}, no obvious fluorescent intensity change was observed. However with the addition of 2.5×10^{-5}mol L^{-1} S^{2-}, the fluorescence intensity decreased at ca. 30%.

Analytical application

Optimal experimental condition

The effect of pH on the luminescence of ZnS:Mn^{2+} was investigated and presented in Fig. 7a. When pH value was lower than 9.0 and higher than 7.0, the intensity of QDs was strong and kept constant and the system was stable at room temperature for at least 3 days. In addition, the effect of pH value on the intensity of QDs-S^{2-} was also studied (shown in Fig. 7b). The intensity stabilized in the pH range of 6.7 to 10.4. In the strong acid the interaction between QDs and S^{2-} was weak because sulfur existed in the form of HS^- instead of S^{2-}. At the same time, the response was also weak in strong base medium because the existence of too much OH^- groups on the surface of QDs hindered the interaction between S^{2-} and QDs. In order to make it feasible, Tris-HCl buffer of pH 7.8 was selected.

At the same time, the effect of concentration of ZnS:Mn^{2+} on the sensitivity was also studied. The fluorescent intensity increased with the increase of concentration of ZnS:Mn^{2+}. However, the degree of fluorescent intensity upon addition of S^{2-} was decreased with the concentration of ZnS:Mn^{2+}. Take both into consideration, the concentration of ZnS:Mn^{2+} was 30 μg mL^{-1}.

Thus, the optimal experiment condition was under room temperature in Tris-HCl buffer of pH 7.8 and the concentration of QDs was 30 μg mL^{-1}.

Interference of foreign substances

Under optimal experimental condition, in the mixture solution of 5.0×10^{-6}mol L^{-1} S^{2-} and 30 μg mL^{-1} QDs, the presence of following amounts of foreign substances compared with the concentration of S^{2-} resulted in less than ±5% error: 1,000-fold NO_3^-, Na^+, K^+, Li^+ and NH_4^+, 600-fold SO_3^{2-}, 500-fold CO_3^{2-}, ClO_4^- and F^-, 400-fold NO_2^- and SO_4^{2-}, 300-fold Br^-, 100-fold I^-, $CH_3CO_2^-$, 20-fold Mg^{2+}, Ca^{2+}, Ba^{2+}. The presence of heavy metal ions such as Cu^{2+}, Hg^{2+} and Ag^+ also quenched the fluorescence of QDs, because the insoluble sulfides formation between metal ions and S^{2-} led to ZnS precipitation transfer which resulted in the change of photophysical properties or the surface state of thiol-capped QDs [32]. However, those ions of high concentration couldn't coexist with S^{2-}, their existence didn't interfere the determination.

Sample analysis

To investigate the possibility of practical application, the determination of sulfide anion was performed on a lake water sample. The recovery was about 103% shown in Table 1.

Table 1 Analytical results of samples

Sample	Found ($mol\cdot L^{-1}$)	Added (10^{-6}molL^{-1})	Found (n=5) ($10^{-6}mol\cdot L^{-1}$)	Recovery (%)	Relative standard deviation (RSD) (%)
Lake water	No found	5.00	5.22	103.3	5.65
		10.0	10.38	103.8	2.77

Proposed mechanism

ZnS dopped Mn^{2+} quantum dots emit two emission bands peaked at 400 nm and 590 nm. The emission at 400 nm originated from the defect-related emission of the ZnS [54] and the emission of 590 nm is attributed to the $^4T_1$–$^6A_1$ transition of Mn^{2+} impurity [48]. When S^{2-} was adsorbed on the surface of the QDs, S^{2-} vacancy of the surface of QDs decreased. As the result, surface fluorescence of ZnS was quenched effectively. At the same time, the adsorption of S^{2-} increased dangling bonds originating from the lone pairs on surface S^{2-} which resulted in more no-radiation pathways of luminescent center, consequently the fluorescence of Mn^{2+} was quenched as well [55].

Since the surface of QDs was coated with negatively charged mercaptoacetic ions, it was very difficult for other anions to interact with the surface of the QDs. However S^{2-} could fit well the sulfide defect of the surface and S^{2-} could bind strongly with Zn^{2+}, thus S^{2-} could easily interact with the QDs [40]. Therefore, QDs showed highly selective response to sulfide anion than other anions.

Conclusions

Water-soluble Mn^{2+}-doped ZnS quantum dots (QDs) were prepared which showed selective response to sulfide anion over other anions such as F^-, Cl^-, Br^-, I^-, $CH_3CO_2^-$, ClO_4^-, CO_3^{2-}, NO_2^-, NO_3^-, $S_2O_3^{2-}$, SO_3^{2-} and SO_4^{2-}. The high selectivity was assumed that S^{2-} could fit well the sulfide defect of the QDs surface and S^{2-} could bind strongly with Zn^{2+}.

Acknowledgements The authors gratefully acknowledge the financial support of this study by Natural Science Foundation of China (No.20965006) and Jiangxi Province Education Ministry Foundation (No.GJJ09040).

References

1. Puacz W, Szahun W (1995) Catalytic determination of sulfide in blood. Analyst 120(3):939–941
2. Hendrickson RG, Chang A, Hamilton RJ (2004) Co-worker fatalities from hydrogen sulfide. Am J Ind Med 45(4):346–350
3. Lawrence NS, Davis J, Compton RG (2000) Analytical strategies for the detection of sulfide: a review. Talanta 52(5):771–784
4. Huang RF, Zheng XW, Qu YJ (2007) Highly selective electrogenerated chemiluminescence (ECL) for sulfide ion determination at multi-wall carbon nanotubes-modified graphite electrode. Anal Chim Acta 582(2):267–274
5. Balasubramanian S, Pugalenthi V (2000) A comparative study of the determination of sulphide in tannery waste water by ion selective electrode (ISE) and iodimetry. Water Res 34(17):4201–4206
6. Ferrer L, de Armas G, Miró M, Estela JM, Cerdà V (2004) A multisyringe flow injection method for the automated determination of sulfide in waters using a miniaturised optical fiber spectrophotometer. Talanta 64(5):1119–1126
7. Silva MSP, Galhardo CX, Masini JC (2003) Application of sequential injection-monosegmented flow analysis (SI-MSFA) to spectrophotometric determination of sulfide in simulated waters samples. Talanta 60(1):45–52
8. Silva MSP, da Silva IS, Abate G, Masini JC (2001) Spectrophotometric determination of acid volatile sulfide in river sediments by sequential injection analysis exploiting the methylene blue reaction. Talanta 53(4):843–850
9. Pouly F, Touraud E, Buisson JF, Thomas O (1999) An alternative method for the measurement of mineral sulphide in waste water. Talanta 50(4):737–742
10. Kuban V, Dasgupta PK, Marx JN (1992) Nitroprusside and methylene blue methods for silicone membrane differentiated flow injection determination of sulfide in water and waste water. Anal Chem 64(1):36–43
11. Colon M, Todoli JL, Hidalgo M, Iglesias M (2008) Development of novel and sensitive methods for the determination of sulfide in aqueous samples by hydrogen sulfide generation-inductively coupled plasma-atomic emission spectroscopy. Anal Chim Acta 609(2):160–168
12. Jin Y, Wu H, Tian Y, Chen LH, Cheng JJ, Bi SP (2007) Indirect determination of sulfide at ultratrace levels in natural waters by flow injection on-line sorption in a knotted reactor coupled with hydride generation atomic fluorescence spectrometry. Anal Chem 79 (18):7176–7181
13. Lawrence NS, Deo RP, Wang J (2004) Electrochemical determination of hydrogen sulfide at carbon nanotube modified electrodes. Anal Chim Acta 517(1–2):131–137
14. Spilker B, Randhahn J, Grabow H, Beikirch H, Jeroschewski P (2008) New electrochemical sensor for the detection of hydrogen sulfide and other redox active species. J Electroanal Chem 612 (1):121–130
15. Tsai DM, Kumar AS, Zen JM (2006) A highly stable and sensitive chemically modified screen-printed electrode for sulfide analysis. Anal Chim Acta 556(1):145–150
16. GarcõÂa-Calzada M, MarbaÂn G, Fuertes AB (1999) Potentiometric determination of sulphur in solid samples with a sulphide selective electrode. Anal Chim Acta 380(1):39–45
17. Giuriati C, Cavalli S, Gorni A, Badocco D, Pastore P (2004) Ion chromatographic determination of sulfide and cyanide in real matrices by using pulsed amperometric detection on a silver electrode. J Chromatogr A 1023(1):105–112
18. Divjak B, Goessler W (1999) Ion chromatographic separation of sulfur-containing inorganic anions with an ICP–MS as element-specific detector. J Chromatogr A 844(1–2):161–169
19. Maya F, Estela JM, Cerdá V (2007) Improving the chemiluminescence-based determination of sulphide in complex environmental samples by using a new, automated multi-syringe flow injection analysis system coupled to a gas diffusion unit. Anal Chim Acta 601(1):87–94
20. Safavi A, Karimi MA (2002) Flow injection chemiluminescence determination of sulfide by oxidation with *N*-bromosuccinimide and *N*-chlorosuccinimide. Talanta 57(3):491–500
21. Du JX, Li YH, Lu JR (2001) Investigation on the chemiluminescence reaction of luminol–H_2O_2–S^{2-}/R–SH system. Anal Chim Acta 448(1–2):79–83
22. Choi MF, Hawkins P (1997) Development of sulphide-selective optode membranes based on fluorescence quenching. Anal Chim Acta 344(1–2):105–110
23. Axelrod HD, Cary JH, Bonelli JE, Lodge JP Jr (1969) Fluorescence determination of sub-parts per billion hydrogen sulfide in the atmosphere. Anal Chem 41(13):1856–1858

24. Spaziani MA, Tinani M, Carroll MK (1997) On-line determination of sulfide by the methylene blue method with diode-laser-based fluorescence detection. Analyst 122(12):1555–1557
25. Rodríguez-Fernández J, Costa JM, Pereiro R, Sanz-Medel A (1999) Simple detector for oral malodour based on spectrofluorimetric measurements of hydrogen sulphide in mouth air. Anal Chim Acta 398(1):23–31
26. Yang XF, Wang LP, Xu HM, Zhao ML (2009) A fluorescein-based fluorogenic and chromogenic chemodosimeter for the sensitive detection of sulfide anion in aqueous solution. Anal Chim Acta 631(1):91–95
27. Wang Q, Kun YC, Wang YW, Shin G, Ruengruglikit C, Huang QR (2006) Luminescent properties of water-soluble denatured bovine serum albumin-coated CdTe quantum dots. J Phys Chem B 100(34):16860–16866
28. Chen YF, Rosenzweig Z (2002) Luminescent CdS Quantum dots as selective ion probes. Anal Chem 74(19):5132–5138
29. Li J, Mei F, Li WY, He XW, Zhang YK (2008) Study on the fluorescence resonance energy transfer between CdTe QDs and butyl-rhodamine B in the presence of CTMAB and its application on the detection of Hg(II). Spectrochimica Acta Part A 70(4):811–817
30. Wu HM, Liang JG, Han HY (2008) A novel method for the determination of Pb^{2+} based on the quenching of the fluorescence of CdTe quantum dots. Microchim Acta 161(1–2):81–86
31. Ruedas-Rama MJ, Hall EAH (2008) Azamacrocycle activated quantum dots for zinc ion detection. Anal Chem 80(21):8260–8268
32. Liang JG, Ai XP, He ZK, Pang DW (2004) Functionalized CdSe quantum dots as selective silver ion chemodosimeter. Analyst 129 (7):619–622
33. Li HB, Zhang Y, Wang XQ (2007) L-Carnitine capped quantum dots as luminescent probes for cadmium ions. Sensors and Actuators B 127(2):593–597
34. Kar S, Banerjee S, Santra S (2008) A simple strategy for quantum dot assisted selective detection of cadmium ions. Chem Commun 26:3037–3039
35. Ali EM, Zheng YG, Yu H, Ying JY (2007) Ultrasensitive Pb^{2+} detection by glutathione-capped quantum dots. Anal Chem 79 (24):9452–9458
36. Lakowicz JR, Gryczynski I, Gryczynski Z, Murphy CJ (1999) Luminescence spectral properties of CdS nanoparticles. J Phys Chem B 103(36):7613–7620
37. Jin WJ, Costa-Fernández JM, Pereiro R, Sanz-Medel A (2004) Surface-modified CdSe quantum dots as luminescent probes for cyanide determination. Anal Chim Acta 522(1):1–8
38. Jin WJ, Fernandez-Arguelles MT, Cosat-fernandez JM, Pereiro R, Sanz-Medel A (2005) Photoactivated luminescent CdSe quantum dots as sensitive cyanide probes in aqueous solutions. Chem Commun 7:883–885
39. Liu X, Guo L, Cheng LX, Ju HX (2009) Determination of nitrite based on its quenching effect on anodic electrochemiluminescence of CdSe quantum dots. Talanta 78(3):691–694
40. Wu CL, Zhao YB (2007) CdS quantum dots as fluorescence probes for the sensitive and selective detection of highly reactive HSe^- ions in aqueous solution. Anal Bioanal Chem 388(3):717–722
41. Mulrooney RC, Singh N, Kaur N, Callan JF (2009) An "off-on" sensor for fluoride using luminescent CdSe/ZnS quantum dots. Chem Commun (6):686–688
42. Norman TJ, Magana JD, Wilson T, Burns C, Zhang JZ (2003) Optical and Surface structural properties of Mn^{2+}-dopped ZnSe nanoparticles. J Phys Chem B 107(26):6309–6317
43. Mahamuni S, Lad AD, Patole S (2008) Photoluminescence properties of manganese-dopped zinc selenide quantum dots. J Phys Chem C 112(7):2271–2277
44. Sapra S, Prakash A, Ghangrekar A, Perasamy N, Sarma DD (2005) Emission properties of manganese-dopped ZnS nanocrystals. J Phys Chem B 109(5):1663–1668
45. Quan ZW, Wang ZL, Yang PP, Lin J, Fang JY (2007) Synthesis and characterization of high-quality ZnS, ZnS:$Mn^{2+}$and ZnS:Mn^{2+}/ZnS (core/shell) luminescent nanocrystals. Inorg Chem 46(4):1354–1360
46. Wang XF, Xu JJ, Chen HY (2008) A new electrochemiluminescence emission of Mn^{2+}-dopped ZnS nanocrystals in aqueous solution. J Phys Chem C 112(45):17581–17585
47. Dong CQ, Qian HF, Fang NH, Ren JC (2006) Study of fluorescence quenching and dialysis process of CdTe quantum dots, using ensemble techniques and fluorescence correlation spectroscopy. J Phys Chem B 110(23):11069–11075
48. Tu RY, Liu BH, Wang ZY, Gao DM, Wang F, Fang QL, Zhang ZP (2008) Amine-capped ZnS:Mn^{2+} nanocrystals for fluorescence detection of trace TNT explosive. Anal Chem 80 (9):3458–3465
49. He Y, Wang HF, Yan XP (2008) Exploring Mn-doped ZnS quantum dots for the room-temperature phosphorescence detection of enoxacin in biological fluids. Anal Chem 80(10):3832–3837
50. Wang HF, He Y, Ji TR, Yan XP (2009) Surface molecular imprinting on Mn-Doped ZnS quantum dots for room-temperature phosphorescence optosensing of pentachlorophenol in water. Anal Chem 81(4):1615–1621
51. Santra S, Yang H, Holloway PH, Stanley JT, Mericle RA (2005) Synthesis of water-dispersible fluorescent, radio-opaque, and paramagnetic CdS:Mn/ZnS quantum dots: A multifunctional probe for bioimaging. J Am Chem Soc 127(6):1656–1657
52. Zhuang JQ, Zhang XD, Wang G, Li DM, Yang WS, Li TJ (2003) Synthesis of water-soluble ZnS:Mn^{2+} nanocrystals by using mercaptopropionic acid as stabilizer. J Mater Chem 13(7):1853–1857
53. Brus LE (1984) Elctron-electron and electron-hole interactions in small semiconductor crystallites: The size dependence of the lowest excited electronic state. J Chem Phys 80(9):4403–4409
54. Sooklal K, Cullum BS, Angel SM, Murphy CJ (1996) Photophysical properties of ZnS nanoclusters with spatially localized Mn^{2+}. J Phys Chem 100(11):4551–4555
55. Chen L, Zhang JH, Luo YS, Lu SZ, Wang XJ (2004) Effect of $Zn^{2+}$and Mn^{2+} introduction on the luminescent properties of colloidal ZnS:Mn^{2+} nanoparticles. Applied Phys Lett 84(1):112–114